Table 1 | A list of miRNAs which were up-regulated more than 2.0-fold by resveratrol in MDA-MB-231-luc-D3H2LN cells compared with control

miRNA	Fold change
Tumor-suppressive miRNA	
hsa-miR-141	4.48
hsa-miR-26a	2.33
hsa-miR-195	3.38
hsa-miR-126	2.41
hsa-miR-185	2.75
hsa-miR-340	11.07
hsa-miR-128	2.13
hsa-miR-34a	2.65
hsa-miR-193b	2.58
hsa-miR-335	2.42
hsa-miR-200c	3.47
hsa-miR-196a	2.67
hsa-miR-497	4.60
hsa-miR-125a-3p	3.00
Onco- miRNA	
hsa-miR-378*	4.81
hsa-miR-10b	5.11
hsa-miR-132	7.23
hsa-miR-222	2.40

contrast, the CSC population was decreased (Fig. 1b). To show direct evidence of whether multiple phenotypes induced by resveratrol were regulated by tumour-suppressive miRNAs, MDA-MB-231-luc-D3H2LN cells were transfected with an antisense oligonucleotide targeting miR-141 (i.e., a miR-141 inhibitor) in the presence of resveratrol treatment. MiR-141 repression by the miR-141 inhibitor was confirmed by qRT-PCR (supplementary Fig. 7a). As shown in Fig. 3a, the miR-141-induced inhibition of invasion was abrogated by the addition of the miR-141 inhibitor, and the MDA-MB-231-luc-D3H2LN cell invasiveness was increased. To confirm the link between resveratrol and miRNA expression, we investigated the growth of breast cancer cells in the presence or absence of a miR-143 inhibitor[27]. In the presence of resveratrol, miR-143-induced inhibition significantly increased the survival of MDA-MB-231-luc-D3H2LN cells relative to the control (Fig. 3b). It has been shown that miR-200c up-regulation in breast cancer cells inhibits Zeb1 expression, resulting in E-cadherin induction in breast cancer cell lines[28]. As shown in Fig. 1d, we found miR-200c up-regulation after resveratrol treatment, suggesting that resveratrol treatment activates this pathway and demonstrating its anti-cancer activity. Indeed, resveratrol addition significantly suppressed Zeb1 expression in the breast cancer cell lines (Fig. 3c) and induced E-cadherin expression in those cells (supplementary Fig. 7b). Furthermore, to show the direct effects of resveratrol on the miRNA machinery, we performed a Zeb1 3′UTR assay and demonstrated that resveratrol treatment significantly down-regulated the luciferase activity of a plasmid containing the Zeb1 3′UTR (Fig. 3d). Taken together, these results suggested that resveratrol plays an important role in breast cancer prevention by up-regulating tumour-suppressive miRNAs.

The stilbene family regulates miRNA biogenesis. The naturally occurring dimethylether resveratrol analogue pterostilbene is a stilbene family member that is generated by plants. Pterostilbene has also been reported to possess chemopreventive activity in cancer and other resveratrol-like health benefits[29,30]. To determine whether pterostilbene induced the expression of tumour-suppressive miRNAs in a similar manner as resveratrol, we assessed the effect of pterostilbene on miRNA expression. As shown in Fig. 4a, pterostilbene treatment suppressed cell growth more significantly than resveratrol treatment in MDA-MB-231-luc-D3H2LN cells. In addition, the expression of tumour suppressive miRNAs (i.e., miR-143 and miR-200c) and Ago2 was significantly higher in pterostilbene-treated MDA-MB-231-luc-D3H2LN cells than in resveratrol-treated cells (Figs. 4b-d and Supplementary Fig. 8). Taken together, these results suggest that resveratrol-induced tumour-suppressive miRNA expression and its anti-cancer activity are conserved among stilbene family members (Fig. 4e).

Discussion

Resveratrol exhibits strong anti-oxidant activity and is capable of inducing apoptosis in cancer cells. Therefore, resveratrol is believed to be efficacious at multiple carcinogenesis stages[4]. However, the underlying molecular mechanism of its anti-tumour activity has yet to be defined. In this study, we demonstrated that resveratrol up-regulated tumour-suppressive miRNAs, resulting in the induction of an anti-cancer effect against the CSC phenotype in cancer cells. We also demonstrated that resveratrol inhibited the invasiveness of breast cancer cells as one of the CSC phenotypes by activating miR-141 and miR-200c. However, the reason why resveratrol reduces the CSC population remains elusive. Recent studies have provided evidence that miR-200c strongly inhibits the ability of breast CSCs to form tumours *in vivo*[31]. These findings suggest that resveratrol shows multiple anti-cancer effects by reducing the CSC population through miR-200c activation.

Argonaute proteins are widely expressed and are involved in post-transcriptional gene silencing. Using microarrays to compare control and Ago2$^{-/-}$ cells, recent studies have demonstrated that Ago2 loss results in the global reduction of mature miRNAs in erythroblasts, fibroblasts, and hepatocytes[32]. However, it has not been determined whether Ago2 alterations can contribute to miRNA expression and the RNAi response. In this study, we show that Ago2 up-regulation by resveratrol leads to an increase in tumour-suppressive miRNAs and the enhancement of RNAi activity.

Pterostilbene has anti-diabetic properties and has been shown to be cytotoxic to a number of cancer cell lines *in vitro*[29,30]. Although pterostilbene and resveratrol have similar pharmacological properties, pterostilbene contains two methoxy groups and one hydroxyl group, while resveratrol has three hydroxyl groups (Supplementary Fig. 9). A recent study demonstrated that pterostilbene shows 95% bioavailability when orally administered, while resveratrol only has 20% bioavailability[33]. Furthermore, pterostilbene is a more powerful chemopreventive agent than resveratrol in colon cancer[34], showing that pterostilbene has several key advantages over resveratrol. In this study, we demonstrate that pterostilbene is more reliable than resveratrol in mediating the anti-cancer effect by inducing tumour-suppressive miRNAs and Ago2 expression. The reason for the difference in the anti-cancer activity of pterostilbene and resveratrol in cancer cells may be due to the expressed miRNAs.

It has been demonstrated that most tumours are characterised by globally diminished miRNA expression[16,17,35]. Thus, the delivery of tumour suppressive miRNAs may allow for the therapeutic restitution of physiological regulation programs lost in cancer and other disease states. However, miRNA therapy shares many of the disadvantages of other treatment approaches including delivery limitations and instability. Therefore, novel methods are required to resolve these issues. Based on this study, we hypothesise that the down-regulation of miRNAs in cancer cells is compensated by resveratrol, which induces the derepression of tumour suppressive miRNAs. Down-regulation of oncogenic miRNAs and up-regulation of tumour-suppressive miRNAs by resveratrol in prostate cancer cells has been reported[36]; however, the connection between resveratrol and the miRNA biogenesis machinery has not been investigated in detail. In this report, we demonstrated that resveratrol leads to a reduction in malignancy by not only activating tumour-suppressive miRNA transcription (Figs. 1d and 2b) but also enhancing the RNAi activity mediated by Ago2 induction (Figs. 2d, e, f and g). Our

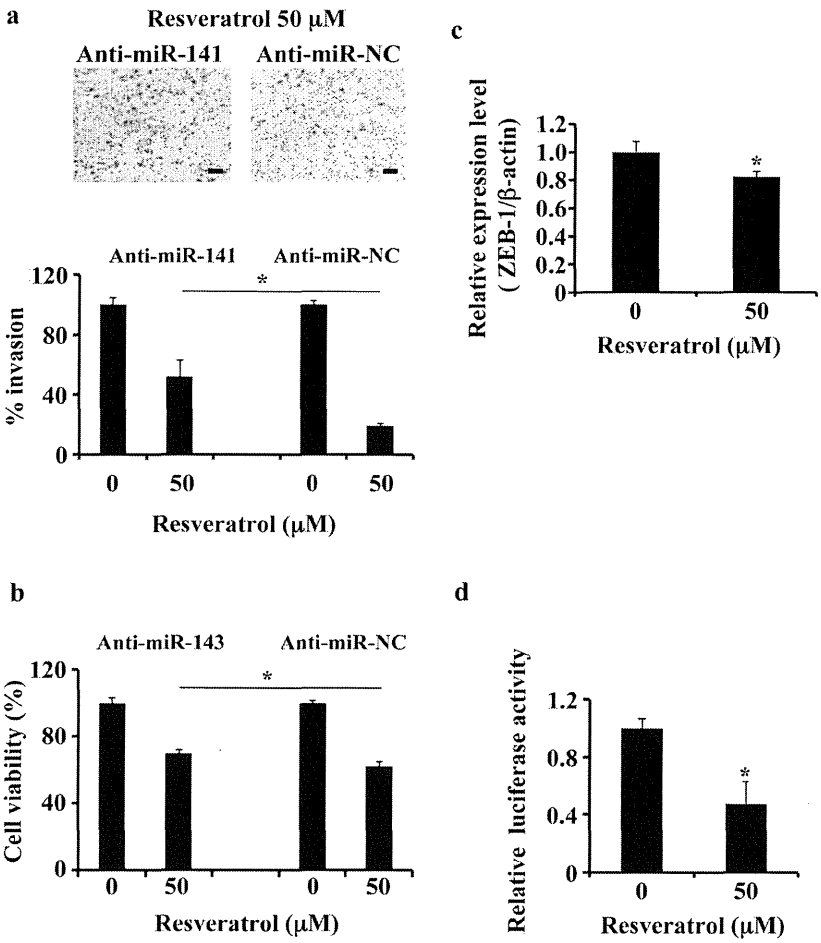

Figure 3 | Multiple anti-cancer effects of tumour-suppressive miRNAs induced by resveratrol. (a) MDA-MB231-luc-D3H2LN cells were grown and transiently transfected with anti-miR-141 or anti-miR-NC (control). After 4 hours, the cells were treated with resveratrol or DMSO (control) for 1 day and subjected to an invasion assay. Representative photographs (upper panel) and quantification (lower panel) are shown. Scale bar: 100 μm. (b) MDA-MB231-luc-D3H2LN cells were cultured and transiently transfected with anti-miR-143 or anti-miR-NC (control). After 4 hours, the cells were treated with resveratrol or DMSO (control) for 72 hours, and the cell viability was measured by the MTS assay. (c) MDA-MB231 cells were treated with resveratrol or DMSO (control). After 2 days of culture, the cell extract was subjected to real-time mRNA qRT-PCR. (d) MDA-MB231 cells were grown and transiently transfected with a ZEB-1 3′UTR or psiCheck2 vector (control) under resveratrol treatment. After 1 day of culture, the cells were subjected to a luciferase reporter assay. The values on the *y-axis* are depicted relative to the luciferase activity of cells treated with DMSO, which is defined as 1 (all data are shown as the mean ± s.e.m., *$P<0.05$).

demonstration that resveratrol potently suppresses even a severe and multifocal carcinogenesis model in the absence of measurable toxicity provides proof of the principle that miRNA replacement by resveratrol may be a clinically viable anti-cancer therapeutic strategy.

In conclusion, this study shows that an orally available small molecule can safely reduce many of the negative consequences at doses acceptable in humans with an overall improvement in health and survival. Our results raise the possibility that the regulation of tumour-suppressive miRNAs by natural agents could be a novel strategy in the design of combinational approaches using conventional therapies for tumour recurrence prevention and in achieving successful treatment outcomes in patients with cancer.

Methods

Reagents. Trans-resveratrol (98% purity) was purchased from Cayman Chemical, pterostilbene (98% purity) from Tokyo Chemical Industry, cycloheximide solution and 5, 6-dichlorobenzimidazole riboside from sigma, and docetaxel from Sanofi-Aventis. The antibiotic solution (containing 10,000 U/mL penicillin and 10 mg/mL streptomycin), the trypsin-EDTA mixture (containing 0.05% trypsin and EDTA), and FBS (fetal bovine serum) were obtained from Invitrogen. The FITC-conjugated anti-CD44 (clone L178) antibody was obtained from Becton Dickinson, and the APC- conjugated anti-CD24 (clone ML5) antibody, from Biolegend. The duplexes of each small interfering RNA (siRNA), targeting human Ago2 mRNA (siAgo2-1, GCACGGAAGUCCAUCUGAAUU, UUCAGAUGGACUUCCGUGCUU; siAgo2-2, GCAGGACAAAGAUGUAUUAUU, UAAUACAUCUUUGUCCUGCUU; siAgo2-3, GGGUCUGUGGUGAUAAAUAUU, UAUUUAUCACCACAGACCCUU; siAgo2-4, GUAUGAGAACCCAAUGUCAUU, UGACAUUGGGUUCUCAUACUU) and negative control 1 were purchased from Applied Biosystems[37].

Plasmids. The primary-miR-143 expression vector was purchased from TaKaRa BIO. The full-length human Ago2 cDNA was cloned into pIRES2-EGFP vector (Clontech). We amplified the upstream of human Ago2 gene (−1,770/−1 relative to the TSS) by PCR using human genomic DNA as template, and we cloned it into the pGL3-Basic vector. For the 3′UTR reporter plasmids, the nucleotides +3,399 to +3,953 of human ZEB1 cDNA were amplified and cloned downstream of the luciferase gene in the psiCHECK2 vector (Promega). For cloning the following primers were used for PCR: Ago2 promoter: 5′-ACGCGTATAGGGGATATGTGAAGGAGACA-3′ (forward) and 5′-CTCGAGATA CGCGCGCGCCACGGGCCCCG-3′ (reverse); ZEB1 3′UTR Fragment: 5′-ATAATACGCGTTAAAGGAAGCTGATTAATTAGATATGC-3′ (forward) and 5′-ATAATAAGCTTTTTGTAGTGCAGAAGTTCTCACATTTT-3′ (reverse)[22].

Cell culture. HEK293 cells (American Type Culture Collection) were cultured in Dulbecco's Modified Eagle's Medium containing 10% heat-inactivated FBS and an antibiotic-antimycotic (Invitrogen) at 37°C in 5% CO_2. MDA-MB-231 cells (American Type Culture Collection) and MDA-MB-231-luc-D3H2LN cells (Xenogen) were cultured in RPMI containing 10% heat-inactivated FBS and antibiotic-antimycotic at 37°C in 5% CO_2. Human mammary carcinoma cell lines, MCF7 cells and multidrug-resistant MCF7-ADR cells were provided by Shien-Lab,

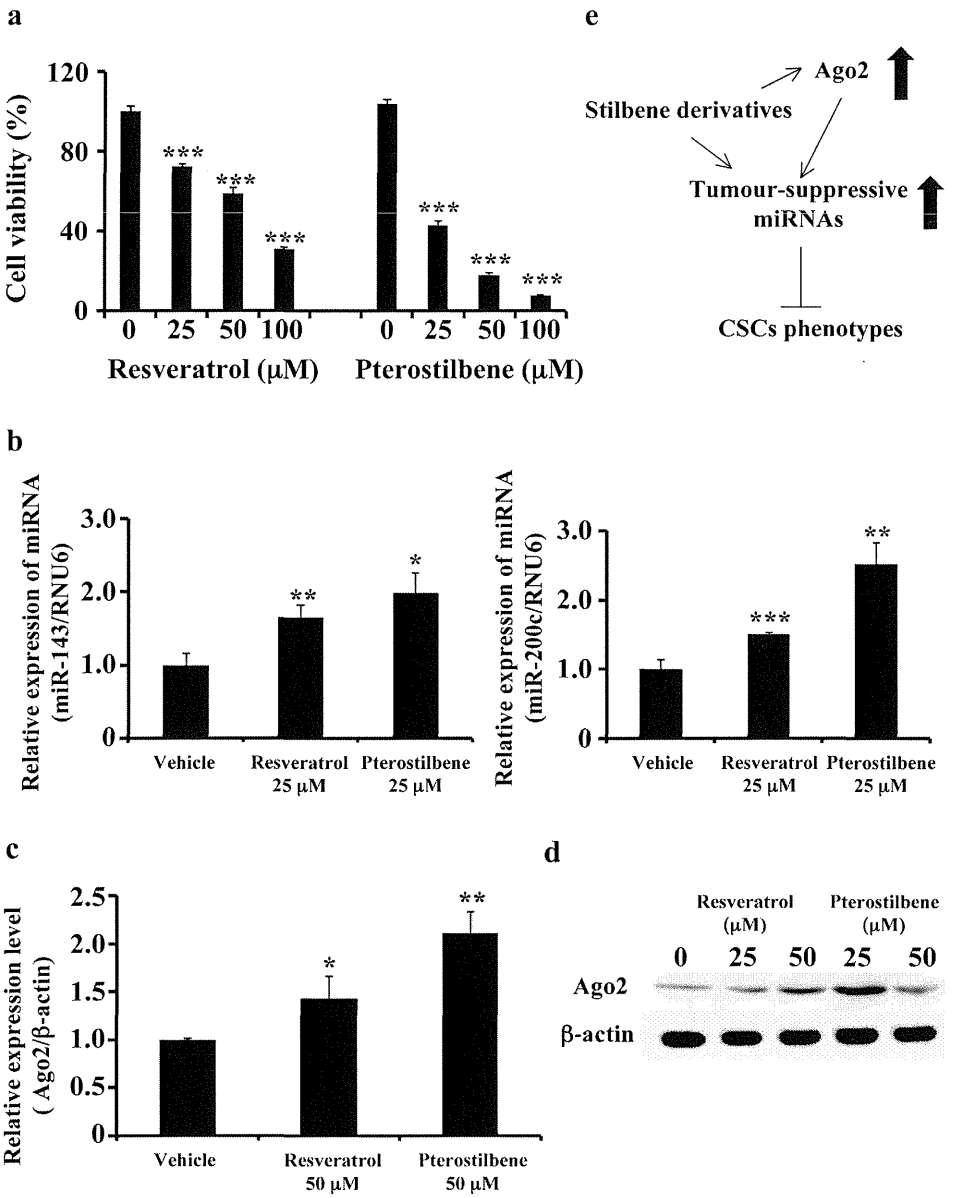

Figure 4 | Effects of pterostilbene on human breast cancer cells. (a) MDA-MB231-luc-D3H2LN cells were cultured in the presence or absence of resveratrol or pterostilbene at the indicated concentrations for 72 hours. Cell viability was measured using the MTS assay. The control wells were treated with DMSO. (b), (c) Expression levels of miR-143, miR-200c (b), and Ago2 (c) in MDA-MB231-luc-D3H2LN cells. The expression levels of the indicated miRNAs were examined in MDA-MB231-luc-D3H2LN cells 48 hours after treatment with pterostilbene. (d) MDA-MB231-luc-D3H2LN cells were treated with stilbenes for 72 hours, and Ago2 expression was detected by immunoblotting. Actin was used as a loading control. (e) Model of the regulation of tumour-suppressive miRNAs and Ago2 expression in the stilbene family (all data are shown as the mean ± s.e.m., *P<0.05, **P<0.01, ***P<0.001).

Medical Oncology, National Cancer Center Hospital of Japan. These cells were maintained in RPMI supplemented with 10% heat-inactivated FBS and antibiotic-antimycotic at 37°C in 5% CO_2. MCF10A cells, which were a spontaneously immortalized nontumorigenic epithelial cell line, (American Type Culture Collection) were maintained in an MEBM medium with 1% GA-1000, 50 μg/ml hydrocortisone, 1 μg/ml hEGF, 500 μg/ml insulin, and 4% BPE (Lonza) at 37°C in 5% CO_2.

Cell proliferation assay (MTS assay). Five thousand cells per well were seeded in 96-well plates. The following day, the cells were treated with resveratrol. After 3 days of culture, cell viability was measured using the Tetra Color One assay kit (Seikagaku Kohgyo) according to the instructions of the manufacturer. The absorbance at 450 nm was measured using Envision (Wallac).

Transwell invasion assay. Breast cancer cell invasion was assayed in 24-well Biocoat Matrigel invasion chambers (8 μm; Becton Dickinson) according to the manufacturer's protocol. Briefly, the cells were treated with resveratrol, and on the following day, 20,000 cells were plated in the upper chamber. The upper chamber contained resveratrol and the bottom chamber contained 10% FBS as a chemoattractant. Twenty-two hours later, the non-invasive cells were removed with a cotton swab. The cells that migrated through the membrane and stuck to the lower surface of the membrane were fixed with methanol and stained with Diff Quick staining. For quantification, the cells were counted under a microscope in four random fields. All assays were performed in triplicate. The data are expressed as the invasion percentage through the Matrigel matrix and membrane relative to migration through the control membrane according to the manufacturer's instructions.

Cell growth inhibition by cytotoxic agents and resveratrol. Breast cancer cells were plated as described above and allowed to attach overnight. The cultures were replenished with fresh medium containing 25 μM resveratrol for 24 hours and then exposed to 2.5 nM of the chemotherapeutic agent docetaxel for an additional 48 hours. Thus, for a single-agent treatment, the cells were exposed to resveratrol or docetaxel for 72 hours. The effect of resveratrol pretreatment on cell viability was examined by the MTS assay method.

Cell sorting and flow cytometric analysis. MDA-MB-231-luc-D3H2LN cells were treated with resveratrol. After culturing for 3 days, MDA-MB-231-luc-D3H2LN cells were suspended in their culture medium and subjected to a JSAN cell sorter (Bay Bioscience). At least one million cells were pelleted by centrifugation at 180 x *g* for 5 minutes at 4°C, resuspended in a 5-μL mixture of a monoclonal mouse anti-human CD44-FITC antibody (Becton Dickinson, clone L178) and a monoclonal mouse anti-human CD24-APC antibody (Biolegend, clone ML5), and incubated for 30 minutes at 4°C. Three independent experiments were performed.

Mammosphere assay. The CD44+/CD24− fraction from MDA-MB-231-luc-D3H2LN cells were resuspended in 1 : 1 DMEM/F12 (Invitrogen) basal medium freshly supplemented with 20 ng/mL human basic fibroblast growth factor (Invitrogen), 20 ng/mL epidermal growth factor (Invitrogen), 10 μg/mL heparin (Sigma-Aldrich), and 1 : 50 B27 supplement without vitamin A (Sigma-Aldrich) and seeded in 10-cm Ultra-Low Attachment Surface plates (Corning) at a density of 5000 cells. Ten days later, the plates were analysed for mammosphere formation.

Tumourigenicity assays in SCID hairless outbred mice. Six-week-old female SCID hairless outbred (SHO) mice were subcutaneously injected with 200 MDA-MB231-luc-D3H2LN cells in 25 μL of PBS and 25 μL of matrigel (n = 5). The mice were then treated with resveratrol (25 mg/kg/day) or ethanol (control) by intraperitoneal injection every day for 8 days. The tumour growth was monitored by injecting luciferin in the mice followed by measuring bioluminescence using an IVIS imaging system. The data were analysed using the LIVINGIMAGE 2.50 software (Xenogen). Six-week-old female SCID Hairless Outbred (SHO) mice were subcutaneously injected with 2000 MDA-MB231-luc-D3H2LN cells in 25 μL of PBS and 25 μL of Matrigel (n = 5). The mice were then treated with resveratrol (25 mg/kg) by intraperitoneal injection (IP) every day for 2 weeks and then with docetaxel (20 mg/kg) by intraperitoneal injection (IP) once per week for 2 weeks. The normalised fold changes (day 22 or day 29/day 15) of bioluminescence emitted from the whole body of the mice are shown. All experimental protocols involving animals were approved by the the Institute for Laboratory Animal Research, National Cancer Center Research Institute.

Isolation of microRNAs. Total RNAs were extracted from cultured cells using the QIAzol and miRNeasy Mini Kit (Qiagen) according to the manufacturer's protocol.

Quantitative Real-Time PCR (qRT-PCR). The qRT-PCR method has been previously described[38]. PCR was performed in 96-well plates using the 7300 Real-Time PCR System (Applied Biosystems). All reactions were performed in triplicate. All of the TaqMan microRNA assays were purchased from Applied Biosystems. hRNU6 was used as an invariant control. SYBR Green I qRT-PCR was performed, and the β-actin housekeeping gene was used to normalise the variation in the cDNA levels. The following pairs of primers were used for gene amplification: for pri-miR-16, 5′-GCAATTACAGTATTTTAAGAGATGAT-3′ (forward) and 5′- CAT-ACTCTACAGTTGTGTTTTAATGT-3′ (reverse); for pri-miR-141-200c, 5′-TGAGCTTGGGACTGCAGAG-3′ (forward) and 5′-CTGAGCCACCTTCCCC-TAC-3′ (reverse); for pri-miR-143, 5′-CAAGGTTTGGTCCTGGGTGCTCAAA-3′ (forward) and 5′-TGGTGGCCTGTGGCGGGACTCCAA-3′ (reverse); for ZEB1, 5′-AAGAATTCACAGTGGAGAGAAGCCA-3′ (forward) and 5′-CGTTTCTTGC-AGTTTGGGCATT-3′ (reverse); for E-cadherin, 5′-GTCCTGGGCAG-ACTGAATTT-3′ (forward) and 5′-GACCAAGAAATGGATCTGTGG-3′ (reverse); and for β-actin, 5′-GGCACCACCATGTACCCTG-3′ (forward) and 5′-CACGG-AGTACTTGCGCTCAG-3′ (reverse)[39].

Quantification of the Ago2 mRNA half-life. MDA-MB231-luc-D3H2LN cells were incubated with 5,6-dichlorobenzimidazole riboside (50 μM), which is an inhibitor of mRNA synthesis. The cells were then treated with 50 μM resveratrol and harvested at the indicated time points. Total cellular RNA was isolated using the RNeasy Mini kit (Qiagen). qRT-PCR analysis of Ago2 mRNA at each time point was performed as described above. The fold-change in the Ago2 mRNA abundance at each time point was determined by the following equation:

Fold change = $2^{-\Delta CT}$, where ΔCT = (CT, Ago2) target - (CT, Ago2) 0 h.

Transient transfection assays. The plasmid transfections were performed using Lipofectamine LTX (Invitrogen). The cell numbers and amount of plasmids for each transfection were determined according to the manufacturer's protocol. The transfection of siRNA and miRNA inhibitors was accomplished using the DharmaFECT transfection reagent (Thermo Scientific) according to the manufacturer's protocol.

Luciferase reporter assay. Cells were seeded in 96-well plates at 3000 cells per well the day before transfection. A total of 500 ng of Ago2 vector, 10 nM siRNA against luciferase and the AllStars negative control were added to each well. The cells were collected 1, 3, or 5 days after transfection and analysed using the Bright-Glo Luciferase Reporter Assay System (Promega).

Immunoblot analysis. SDS-PAGE gels were calibrated using Precision Plus protein standards (161-0375) (Bio-Rad), and anti-Ago2 (1 : 200) and anti-actin (1 : 1,000) were used as the primary antibodies. The dilution ratio of each antibody is indicated in parentheses. A peroxidase-labelled anti-mouse secondary antibody was used at a dilution of 1 : 10,000. Bound antibodies were visualised by chemiluminescence using the ECL Plus Western blotting detection system (RPN2132) (GE HealthCare), and luminescent images were analysed using a LuminoImager (LAS-3000; Fuji Film Inc.).

Quantification of Ago2 protein half-life. MDA-MB-231-luc-D3H2LN cells at 80% confluency were treated with 30 μg/ml cycloheximide (Sigma-Aldrich). The cells were then treated with 50 μM resveratrol and harvested at the indicated time points. The effect of resveratrol on Ago2 stability was examined by immunoblotting as reported above.

Statistical analysis. The data presented in bar graphs are the means ± s.e.m. of at least three independent experiments. Statistical analyses were performed using the Student's t-test.

1. Hartwell, J. L. & Schrecker, A. W. Components of Podophyllin. V. The Constitution of Podophyllotoxin1. *J Am Chem Soc* **73**, 2909–2916 (1951).
2. Baur, J. A. & Sinclair, D. A. Therapeutic potential of resveratrol: the in vivo evidence. *Nat Rev Drug Discov* **5**, 493–506 (2006).
3. Renaud, S. & de Lorgeril, M. Wine, alcohol, platelets, and the French paradox for coronary heart disease. *Lancet* **339**, 1523–1526 (1992).
4. Jang, M. *et al.* Cancer chemopreventive activity of resveratrol, a natural product derived from grapes. *Science* **275**, 218–220 (1997).
5. Fremont, L. Biological effects of resveratrol. *Life Sci* **66**, 663–673 (2000).
6. Hammell, C. M., Lubin, I., Boag, P. R., Blackwell, T. K. & Ambros, V. nhl-2 Modulates microRNA activity in Caenorhabditis elegans. *Cell* **136**, 926–938 (2009).
7. Stefani, G. & Slack, F. J. Small non-coding RNAs in animal development. *Nat Rev Mol Cell Biol* **9**, 219–230 (2008).
8. Kong, D. *et al.* miR-200 regulates PDGF-D-mediated epithelial-mesenchymal transition, adhesion, and invasion of prostate cancer cells. *Stem Cells* **27**, 1712–1721 (2009).
9. Zhao, J. J. *et al.* MicroRNA-221/222 negatively regulates estrogen receptor alpha and is associated with tamoxifen resistance in breast cancer. *J Biol Chem* **283**, 31079–31086 (2008).
10. Takeshita, F. *et al.* Systemic delivery of synthetic microRNA-16 inhibits the growth of metastatic prostate tumors via downregulation of multiple cell-cycle genes. *Mol Ther* **18**, 181–187 (2010).
11. Melkamu, T., Zhang, X., Tan, J., Zeng, Y. & Kassie, F. Alteration of microRNA expression in vinyl carbamate-induced mouse lung tumors and modulation by the chemopreventive agent indole-3-carbinol. *Carcinogenesis* **31**, 252–258 (2010).
12. Tsang, W. P. & Kwok, T. T. Epigallocatechin gallate up-regulation of miR-16 and induction of apoptosis in human cancer cells. *J Nutr Biochem* **21**, 140–146 (2010).
13. Li, Y. *et al.* Up-regulation of miR-200 and let-7 by natural agents leads to the reversal of epithelial-to-mesenchymal transition in gemcitabine-resistant pancreatic cancer cells. *Cancer Res* **69**, 6704–6712 (2009).
14. Sun, M. *et al.* Curcumin (diferuloylmethane) alters the expression profiles of microRNAs in human pancreatic cancer cells. *Mol Cancer Ther* **7**, 464–473 (2008).
15. Lee, H. P. *et al.* Dietary effects on breast-cancer risk in Singapore. *Lancet* **337**, 1197–1200 (1991).
16. Croce, C. M. Causes and consequences of microRNA dysregulation in cancer. *Nat Rev Genet* **10**, 704–714 (2009).
17. Gaur, A. *et al.* Characterization of microRNA expression levels and their biological correlates in human cancer cell lines. *Cancer Res* **67**, 2456–2468 (2007).
18. Al-Hajj, M., Wicha, M. S., Benito-Hernandez, A., Morrison, S. J. & Clarke, M. F. Prospective identification of tumorigenic breast cancer cells. *Proc Natl Acad Sci U S A* **100**, 3983–3988 (2003).
19. Al-Hajj, M. Cancer stem cells and oncology therapeutics. *Curr Opin Oncol* **19**, 61–64 (2007).
20. Al-Hajj, M., Becker, M. W., Wicha, M., Weissman, I. & Clarke, M. F. Therapeutic implications of cancer stem cells. *Curr Opin Genet Dev* **14**, 43–47 (2004).
21. Iorio, M. V. *et al.* MicroRNA gene expression deregulation in human breast cancer. *Cancer Res* **65**, 7065–7070 (2005).
22. Burk, U. *et al.* A reciprocal repression between ZEB1 and members of the miR-200 family promotes EMT and invasion in cancer cells. *EMBO Rep* **9**, 582–589 (2008).
23. Carmell, M. A. & Hannon, G. J. RNase III enzymes and the initiation of gene silencing. *Nat Struct Mol Biol* **11**, 214–218 (2004).
24. Kim, V. N. MicroRNA biogenesis: coordinated cropping and dicing. *Nat Rev Mol Cell Biol* **6**, 376–385 (2005).
25. Lingel, A., Simon, B., Izaurralde, E. & Sattler, M. Structure and nucleic-acid binding of the Drosophila Argonaute 2 PAZ domain. *Nature* **426**, 465–469 (2003).
26. Korpal, M., Lee, E. S., Hu, G. & Kang, Y. The miR-200 family inhibits epithelial-mesenchymal transition and cancer cell migration by direct targeting of E-cadherin transcriptional repressors ZEB1 and ZEB2. *J Biol Chem* **283**, 14910–14914 (2008).
27. Xu, B. *et al.* miR-143 decreases prostate cancer cells proliferation and migration and enhances their sensitivity to docetaxel through suppression of KRAS. *Mol Cell Biochem* **350**, 207–213 (2011).
28. Burk, U. *et al.* A reciprocal repression between ZEB1 and members of the miR-200 family promotes EMT and invasion in cancer cells. *Embo Reports* **9**, 582–589 (2008).

29. Rimando, A. M. *et al.* Cancer chemopreventive and antioxidant activities of pterostilbene, a naturally occurring analogue of resveratrol. *J Agric Food Chem* **50**, 3453–3457 (2002).
30. Stivala, L. A. *et al.* Specific structural determinants are responsible for the antioxidant activity and the cell cycle effects of resveratrol. *J Biol Chem* **276**, 22586–22594 (2001).
31. Shimono, Y. *et al.* Downregulation of miRNA-200c links breast cancer stem cells with normal stem cells. *Cell* **138**, 592–603 (2009).
32. O'Carroll, D. *et al.* A Slicer-independent role for Argonaute 2 in hematopoiesis and the microRNA pathway. *Genes Dev* **21**, 1999–2004 (2007).
33. Kapetanovic, I. M., Muzzio, M., Huang, Z., Thompson, T. N. & McCormick, D. L. Pharmacokinetics, oral bioavailability, and metabolic profile of resveratrol and its dimethylether analog, pterostilbene, in rats. *Cancer Chemother Pharmacol* (2010).
34. Chiou, Y. S. *et al.* Pterostilbene is more potent than resveratrol in preventing azoxymethane (AOM)-induced colon tumorigenesis via activation of the NF-E2-related factor 2 (Nrf2)-mediated antioxidant signaling pathway. *J Agric Food Chem* **59**, 2725–2733 (2011).
35. Chang, T. C. *et al.* Transactivation of miR-34a by p53 broadly influences gene expression and promotes apoptosis. *Mol Cell* **26**, 745–752 (2007).
36. Dhar, S., Hicks, C. & Levenson, A. S. Resveratrol and prostate cancer: Promising role for microRNAs. *Mol Nutr Food Res* **55**, 1219–1229 (2011).
37. Meister, G. *et al.* Human Argonaute2 mediates RNA cleavage targeted by miRNAs and siRNAs. *Mol Cell* **15**, 185–197 (2004).
38. Mitchell, P. S. *et al.* Circulating microRNAs as stable blood-based markers for cancer detection. *Proc Natl Acad Sci U S A* **105**, 10513–10518 (2008).
39. Suzuki, H. I. *et al.* Modulation of microRNA processing by p53. *Nature* **460**, 529–533 (2009).

Acknowledgements

This work was supported in part by a Grant-in-Aid for the Third-Term Comprehensive 10-Year Strategy for Cancer Control, a Grant-in-Aid for Scientific Research on Priority Areas Cancer from the Ministry of Education, Culture, Sports, Science and Technology, the National Cancer Center Research and Development Fund, the Program for Promotion of Fundamental Studies in Health Sciences of the National Institute of Biomedical Innovation (NiBio), Project for Development of Innovative Research on Cancer Therapeutics, and the Japan Society for the Promotion of Science (JSPS) through the "Funding Program for World-Leading Innovative R&D on Science and Technology (FIRST Program)" initiated by the Council for Science and Technology Policy (CSTP). We thank Ayako Inoue for excellent technical assistance. We thank Dr.Izuho Hatada for providing the information about Ago2 promoter region.

Author contributions

TO supervised the project. KH performed a significant amount of the experimental work. TO, KH, NK, and YY wrote the manuscript and prepared the figures and tables. *In vivo* experiments were carried out by KH, NK, YY, RT, and FT.

Additional information

Supplementary information accompanies this paper at http://www.nature.com/scientificreports

Competing financial interests: The authors declare no competing financial interests.

How to cite this article: Hagiwara, K. *et al.* Stilbene derivatives promote Ago2-dependent tumour-suppressive microRNA activity. *Sci. Rep.* **2**, 314; DOI:10.1038/srep00314 (2012).

STEM CELLS®

CANCER STEM CELLS

LGR5-Positive Colon Cancer Stem Cells Interconvert with Drug Resistant LGR5-Negative Cells and are Capable of Tumor Reconstitution

Shinta Kobayashi[a, b], Hisafumi Yamada-Okabe[b], Masami Suzuki[b], Osamu Natori[a, b], Atsuhiko Kato[b], Koichi Matsubara[a, b], Yu Jau Chen[a], Masaki Yamazaki[b], Shinichi Funahashi[c], Kenji Yoshida[c], Eri Hashimoto[d], Yoshinori Watanabe[d], Hironori Mutoh[d], Motooki Ashihara[d], Chie Kato[b], Takeshi Watanabe[b], Takashi Yoshikubo[b], Norikazu Tamaoki[e], Takahiro Ochiya[f], Masahiko Kuroda[g], Arnold J. Levine[h], Tatsumi Yamazaki[c,i]

[a] PharmaLogicals Research Pte. Ltd., Singapore; [b] Gotemba Research Laboratories, Chugai Pharmaceutical Co., Ltd., Japan; [c] Forerunner Pharma Research Co., Ltd., Japan; [d] Kamakura Research Laboratories, Chugai Pharmaceutical Co., Ltd., Japan; [e] Central Institute for Experimental Animals, Japan; [f] Division of Molecular and Cellular Medicine, National Cancer Center Research Institute, Japan; [g] Department of Molecular Pathology, Tokyo Medical University, Japan; [h] Institute for Advanced Study, Princeton, USA.; [i] Chugai Pharmaceutical Co., Ltd., Japan

Key words. Cancer stem cells • Drug target • Experimental models • Monoclonal antibodies • Colon cancer • Lgr5

ABSTRACT

The cancer stem cell (CSC) concept has been proposed as an attractive theory to explain cancer development, and CSCs themselves have been considered as targets for the development of diagnostics and therapeutics. However, many unanswered questions concerning the existence of slow cycling/quiescent, drug resistant CSCs remain. Here we report the establishment of colon cancer CSC lines, interconversion of the CSCs between a proliferating and a drug resistant state, and reconstitution of tumor hierarchy from the CSCs. Stable cell lines having CSC properties were established from human colon cancer after serial passages in NOD/Shi-*scid*, IL-2Rγ^{null} (NOG) mice and subsequent adherent cell culture of these tumors. By generating specific antibodies against LGR5, we demonstrated that these cells expressed LGR5 and underwent self-renewal using symmetrical divisions. Upon exposure to irinotecan, the LGR5$^+$ cells transitioned into an LGR5$^-$ drug resistant state. The LGR5$^-$ cells converted to an LGR5$^+$ state in the absence of the drug. DNA microarray analysis and immunohistochemistry demonstrated that HLA-DMA was specifically expressed in drug resistant LGR5$^-$ cells and epiregulin was expressed in both LGR5$^+$ and drug resistant LGR5$^-$ cells. Both cells sustained tumor initiating activity in NOG mice, giving rise to a tumor tissue hierarchy. In addition, anti-epiregulin antibody was found to be efficacious in a metastatic model. Both LGR5$^+$ and LGR5$^-$ cells were detected in the tumor tissues of colon cancer patients. The results provide new biological insights into drug resistance of CSCs and new therapeutic options for cancer treatment.

Author contributions: H.Y.O and T.Ya.: conception and design, data analysis and interpretation, and writing manuscript, final approval of manuscript; S.K., M.S., O.N., A.K., K.M. and T.O.: collection and assembly of data and data analysis and interpretation; Y.J.C., M.Y., E.H., Y.W., H.M., M.A., C.K., and T.W.: collection and assembly of data; T.Yo. N.T. and M.K.: data analysis and interpretation; S.F. and K.Y.: provision of study material (new antibodies); A.J.L.: other (support of manuscript). S. K. and H.Y.O. contributed equally to this article.

Correspondence: Hisafumi Yamada-Okabe Ph.D., Gotemba Research Laboratories, Chugai Pharmaceutical Co., Ltd., 1-135 Komakado, Gotemba, Shizuoka 412-8513, Japan., Telephone: +81-550-87-6709; Fax: +81-550-87-3637; e-mail; okabehsf@chugai-pharm.co.jp; Received April 19, 2012; accepted for publication September 01, 2012. 1066-5099/2012/$30.00/0 doi: 10.1002/stem.1257

This article has been accepted for publication and undergone full peer review but has not been through the copyediting, typesetting, pagination and proofreading process which may lead to differences between this version and the Version of Record. Please cite this article as an 'Accepted Article', doi: 10.1002/stem.1257

INTRODUCTION

Tumors arise from normal tissues by the progression of multiple mutations resulting in malignant cells. The origin of the cells harboring these mutations, whether stem cells, progenitor cells or mature differentiated cells, remains unclear. The heterogeneity of tumor cell types and the prevalence of drug resistance have lead to the hypothesis for the existence of cancer stem cells (CSCs), although this theory is still an ongoing debate [1-7].

Evidence for the existence of colon cancer stem cells has been the most convincing, with LGR5 positive ($LGR5^+$) cells of particular interest in CSC studies [8-12]. Lgr5, a Wnt target gene, was first identified as a marker for normal stem cells in the intestine [13]. It was also reported that Lgr5-positive ($Lgr5^+$) cells formed adenomas upon deletion of Apc and that Lgr5 is expressed in colon cancer cell lines [8]. The cells with high Wnt activity, thereby rendering them $LGR5^+$, are functionally designated colon cancer stem cells [14]. Clearly, LGR5 is an important molecule to identify colon CSCs.

In the normal intestine, Tian et al. described that Lgr5 negative ($Lgr5^-$) stem cells serve as a reserve population of $Lgr5^+$ cells that are themselves therefore dispensable for normal small intestine cell reproduction [15]. It was also reported that slow cycling stem cells (SCs) positive for Hopx are present at the position 4 (the stem cell crypt), and that there is an interconversion between $Hopx^+$ slow cycling SCs and $Lgr5^+$ proliferating SCs located at the crypt base [16]. Similarly in CSCs, several reports suggest the existence of distinct states of CSCs [17-21]. However, it remains unknown how proliferating CSCs acquire a drug resistant phenotype and whether interconversion between proliferating and slow cycling/quiescent CSCs occurs. Difficulties in investigating CSCs are due to the heterogeneity of cell types and the rare presence of CSCs in cancer tissues. Many attempts have been made to enrich and isolate CSCs by spheroid cultures *in vitro*, cell sorting with CSC markers and direct xenotransplantation of cancer cells to immunodeficient mice [22-30]. Although spheroid cultures enrich CSCs, they result in heterogeneous populations of cells and are not efficient enough to isolate and maintain pure CSC populations [14].

Here we report the establishment of human colon cancer cell lines that express LGR5 and possess CSC properties. The cell lines were created using serial passages of colon cancer cells in xenotransplantion in NOD/Shi-*scid,* IL-$2R\gamma^{null}$ (NOG) mice followed by adherent culture of cells. For this purpose, we generated antibodies that are specific to LGR5. The obtained $LGR5^+$ cells transitioned to LGR5-negative ($LGR5^-$) cells upon exposure to an anticancer drug, and such $LGR5^-$ cells reverted to $LGR5^+$ cells after re-seeding and culturing without an anticancer drug. By gene expression profiling of the cell lines, we demonstrated that HLA-DMA, which belongs to the HLA class II alpha chain paralogues, is expressed in drug-resistant $LGR5^-$ cells and epiregulin (EREG), a member of the epidermal growth factor family which can function as a ligand of epidermal growth factor receptor and most members of the ErbB family of tyrosine-kinase receptors, is expressed in both proliferating $LGR5^+$ and drug resistant $LGR5^-$ cells. Using antibodies against LGR5, HLA-DMA and EREG, we show the existence of $LGR5^+$ and $LGR5^-$ cells in xenotransplanted tumor tissues and in human colon cancer tissues from patients. Furthermore, the anti-EREG antibody exhibited antitumor activity against tumors derived from the $LGR5^+$ cells in a metastatic model. This is the first demonstration of the establishment of stable cell lines having CSC properties and the ability to transition between the two distinct states, proliferating and a drug-resistant state. Thus, $LGR5^+$ colon CSCs interconvert with drug resistant $LGR5^-$ cells and are capable of tumor reconstitution. This suggests the physiological importance of CSCs in tumor recurrence after drug treatment. Further, using the anti-EREG antibody, we

provide an option for cancer stem cell targeting therapy.

Materials and Methods

Preparation of monoclonal antibodies against LGR5

Anti-LGR5 monoclonal antibodies, 2L36 and 2U2E-2, were obtained by DNA immunization and protein immunization, respectively. For DNA immunization, plasmid DNA containing *LGR5* was transferred once a week 6 times to the abdominal skin of 6-week-old female MRL/lpr mice (MRL/MpJ-Tnfrsf6<lpr>/Crlj) (Charles River Japan) using a Helicos Gene Gun (BioRad) at a pressure of 200 to 300 psi. At the final immunization, $1x10^6$ cells of CHO DG44 (Life technologies) expressing LGR5 were intravenously injected. The splenocytes were resected 3 days after the final immunization and fused with P3-X63-Ag8U1 mouse myeloma cells (ATCC). 2L36 was obtained by screening the culture supernatants of hybridoma by flow cytometry [31].

The N-terminal region of LGR5 (amino acid 1-555) was expressed as a fusion protein with the Fc region of mouse IgG2a in CHO DG44 cell. The LGR5-Fc protein secreted in the culture medium was purified with HiTrap Protein A FF column (GE Healthcare), and then 6-week-old female Balb/c mice (Charles River Japan) were immunized subcutaneously with 50 μg of the LGR5-Fc protein emulsified in Freund's Complete Adjuvant (Difco). Immunization was repeated once a week for two weeks with the same amount of the LGR5-Fc protein in Freund's Incomplete Adjuvant (Difco). Three days before cell fusion, mice were injected intravenously with 25 μg of the LGR5-Fc protein. Hybridomas were generated as described above, and the antibody 2U2E-2 was selected by ELISA with the LGR5-Fc protein.

Establishment of human colon cancer xenografts using NOG mice

Colon cancer specimens were obtained from consenting patients, as approved by the ethical committee at PharmaLogicals Research and Parkway Laboratory Services in Singapore. Pieces of tumors were minced by scissors and implanted into the flank of NOG mice (Central Institute for Experimental Animals). The human colon cancer xenografts were maintained by passages in NOG mice. All studies and procedures involving animal subjects were approved by the Animal Care and Use Committee at PharmaLogicals Research and the Institutional Animal Care and Use Committee at Chugai Pharmaceutical Co., Ltd. The animals used in this experiment were treated in accordance with the Animal Research Guideline of PharmaLogicals Research and the Guidelines for the Care and Use of Laboratory Animals at Chugai Pharmaceutical Co., Ltd.

Establishment of colon cancer cell lines with cancer stem cell properties

Single cell suspension of cancer cells from the xenografts was prepared by mincing the tissues with scissors, incubated in DPBS containing collagenase/dispase (Roche) and DNase I (Roche) at 37°C for 3 hr followed by filtrating 40 μm cell strainer (BD Biosciences) and suspending in lysing buffer (BD Biosciences). The cells were cultured in a stem cell medium [DMEM/F12 medium (Life technologies) supplemented with N-2 supplement (Life technologies), 20 ng/mL human EGF (Life technologies), 10 ng/mL human basic fibroblast growth factor (Sigma), 4 μg/mL heparin (Sigma), 4 mg/mL BSA (Life technologies), 20 μg/mL human insulin, zinc solution (Life technologies), and 2.9 mg/mL glucose (Sigma)] at 37°C under 5% CO_2 [32]. Culture flasks treated polystyrene (BD Biosciences) and Ultra Low-Attachment cell culture flasks (Corning) were used for adherent cultures and the spheroid cultures, respectively. Drug resistant $LGR5^-$ cells were obtained by treating the adherent $LGR5^+$ cells with 10 μg/mL irinotecan (Hospira) for 3 days.

Sorting of the $LGR5^+$ and $LGR5^-$ cells

The primary cells from xenografts were incubated with the anti-LGR5 antibody (2L36, 2

μg/mL) and then PE-labeled anti-mouse IgG2a (Life technologies, 1/200 dilution). Mouse cells were discriminated from the human colon cancer cells by staining with anti-mouse MHC class I antibody (Abcam, 0.1 μg/mL) and APC-labeled anti-rat IgG (BioLegend, 1/100 dilution). Anti-CD133 antibody (Miltenyi Biotec, 5 μg/mL) and Alexa 488-labeled anti-mouse IgG1 (Life technologies, 1/100 dilution) were used to detect CD133. Dead cells were removed by 7-AAD Viability Dye (Beckman Coulter). Flow cytometry analysis and cell sorting were performed using a MoFlo XDP (Beckman Coulter) cell sorter.

In vitro colony formation assay

To test the colony formation ability, cells were seeded on a layer of 100% matrigel (BD Bioscience) at 10,000 cells/well and cultured in a stem cell medium supplemented with 10% heat-inactivated fetal bovine serum and 5% matrigel.

Tumor formation *in vivo*

Cells suspended in Hank's balanced salt solution (Life technologies) with 50% matrigel were subcutaneously inoculated into the flank of NOG mice. For single cell inoculation, cells were stained with FITC-labeled anti-EpCAM antibody (Miltenyi Biotec) and seeded in Terasaki plates (Thermo Fisher Scientific). After the presence of single cell in each well was confirmed under a fluorescence microscope, the single cell in 50 μL of 50% matrigel was inoculated into the flank of mice. Estimated CSC density was calculated by the formula available on the WEHI ELDA website [33].

Histological examination

Small pieces of surgical specimens of human tissues and of the xenograft tumor tissues were fixed with 4% paraformaldehyde at 4°C for 16 to 24 hr and embedded in paraffin by the AMeX method [34, 35]. After washing the *in vitro* cultured cells with PBS-EDTA, the cells were fixed with 4% paraformaldehyde at 4°C for 2 hr, suspended in 0.5 mL agarose, and embedded in paraffin with AMeX method. Thin sections were subjected to hematoxylin & eosin staining and to immunohistochemisty.

Immunohistochemistry

Thin sections from the above mentioned paraffin blocks were incubated with anti-LGR5 antibody (2U2E-2, 1 μg/mL), anti-EREG antibody (10 μg/mL), anti-E-cadherin antibody (Abcam, 2.5 μg/mL), anti-HLA-DMA antibody (Sigma, 2.5 μg/mL) or FITC-labeled anti-Ki67 antibody (Abcam, 2.5 μg/mL). After the incubation with the primary antibodies, the sections were incubated with a secondary antibody conjugated with polymer-HRP (DAKO or Vector Laboratories) or biotin, and the proteins were visualized by AlexaFluor 488-labeled tyramide (Life technologies, 1/100 dilution), AlexaFluor 568-labeled tyramide (Life technologies, 1/100 dilution), or AlexaFluor 568-labeled streptavidin (Life technologies, 2 μg/mL). For immunofluorescent cytochemistry, cells were fixed with 4% paraformaldehyde and permeabilized with 0.1% Triton-X 100 (Sigma), and incubated with anti-LGR5 antibody (2L36, 2 μg/mL). After the incubation with the primary antibodies, the cells were incubated with AlexaFluor 488-labeled anti-mouse IgG (Life technologies, 1/100 dilution). Those specimens and cells were also stained with DAPI (Life technologies).

Induction of the transition between $LGR5^+$ and $LGR5^-$ states in single cell culture

$LGR5^+$ cells were sorted with an anti-LGR5 antibody, and single $LGR5^+$ cells were cultured in 96-well microplates. To obtain drug resistant $LGR5^-$ cells, $LGR5^+$ cells were treated with 10 μg/mL irinotecan for 3 days. Single $LGR5^-$ cells were cultured in 96-well microplates for 4 days. The medium used for the single cell culture contained 10% conditioned medium of the *in vitro* cultured $LGR5^+$ cells under an adherent condition. $LGR5^+$ and $LGR5^-$ states of the cells were confirmed by immunocytochemical analysis with anti-LGR5 antibody.

Determination of anti-tumor activity of anti-EREG antibody *in vivo*

2 x 10^6 of $LGR5^+$ cells were suspended in Hank's Balanced Sodium Solution and intravenously injected into the tail vein of Fox Chase SCID Beige Mouse (CB17.Cg-$Prkdc^{scid}Lyst^{bg}$/Crl, Charles River). For treatment with the anti-EREG antibody, the mice were intravenously administered 10 mg/kg of anti-EREG antibody once a week for 5 times starting 3 days after tumor inoculation. Mice were scarified 5 days after the final administration under deep anesthesia, and lung tissues were collected. The lung tissues trimmed into 11 pieces were fixed in 4% paraformaldehyde for 24 hr, paraffin embedded by AMeX method [34, 35]. After thin sections were prepared and stained with hematoxylin & eosin, the number of tumors was counted. The sizes of the tumors were determined under a microscope with micrometer.

Statistical analysis

The Mann-Whitney U test was applied to determine the statistical significance of the differences in the numbers of tumor nodules in a metastatic tumor model. The statistical analysis was carried out with an SAS preclinical package (SAS Institute, Inc.). *P* values smaller than 0.05 were considered significant.

RESULTS

Generation and characterization of specific antibodies against LGR5

Having an antibody specific to LGR5 is critical to isolate and characterize colon CSCs, but such antibody has not been available yet. Therefore, we first attempted to generate anti-LGR5 antibodies that enable us to isolate and analyze cells having colon CSC properties. Two monoclonal antibodies, 2L36 and 2U2E-2, specific to LGR5 were obtained. The regions of the LGR5 protein that contain epitopes of these antibodies are shown in Fig. 1A. Both antibodies were tested for immunohistochemistry and flow cytometry using the CHO cells expressing highly related proteins LGR4, LGR5, or LGR6. When used for immunostaining, both 2L36 and 2U2E-2 recognized CHO cells expressing LGR5 but not those expressing LGR4 or LGR6 (Fig. 1B). In flow cytometry analysis, only 2L36 strongly reacted with CHO cells expressing LGR5 (Fig. 1C). Moreover, the antibody 2U2E-2 reacted specifically with crypt base columnar cells in the normal human intestine (Fig. 1D and Supporting Information Fig. S1A). There was also a good correlation between mRNA expression and cell surface staining of the anti-LGR5 antibody in human colon cancer cell lines, which included the CSC lines established in this study and six commercially available lines (Supporting Information Fig. S1B).

Establishment of human colon cancer cell lines with cancer stem cell properties

We established 11 human colon cancer xenografts using NOG mice [36]. Ten out of 11 xenografts were derived from moderately differentiated colon cancer, and one was from poorly differentiated colon cancer. Both the moderately differentiated colon cancer xenografts and the poorly differentiated colon cancer xenograft reconstituted almost the same histological morphologies as the original tumors; the moderately differentiated colon cancer xenografts formed clear epithelial ducts and small budding clusters. In contrast, the poorly differentiated colon cancer xenograft showed no clear epithelial duct structure. We used two moderately differentiated colon cancer xenografts, namely PLR59 and PLR123, for the establishment of colon CSC lines. PLR59 and PLR123 were heterozygous for the mutant K-Ras (G12D), and PLR123 carried the mutant p53 (R249M) in one allele. These xenografts were chosen because they grew faster while retaining the ability to reconstitute tumors with epithelial ducts and small budding clusters even after ten passages in NOG mice (Fig. 1E). In the epithelial ducts of the tumors, differentiated cancer cells that showed goblet cell-like phenotype were also observed in the xenotransplanted tumor tissues throughout the passages (Fig. 1E inset).

To confirm the existence of CSCs in the xenotransplanted tumor tissues, we employed immunohistochemical staining for the LGR5 protein that marks colon CSCs. $LGR5^+$ cells were detected in the original tumor tissues of PLR59 and PLR123 and in their xenotransplanted tumor tissues throughout the passages (Fig. 1F). The frequency of $LGR5^+$ cells in the original tumor tissues was quite low: it was approximately 0.01% in PLR59 and approximately 0.04% in PLR123. In the xenotransplanted tumor tissues, the frequency of $LGR5^+$ cells increased during the passages (Fig. 1F). Tumor initiating activity (TIA) of the primary cells from the PLR123 xenografts was also increased after the passages. The estimated percentage of CSC in the primary cells, as judged from TIA, was approximately 0.1% after 5 passages, and after 14 passages it increased to approximately 0.4% (Supporting Information Table S1). Schematic representation of the establishment of the colon cancer cell lines is shown in Fig. 2A.

Cancer stem cell properties of the established colon cancer cell lines

The major properties of CSCs are self-renewal, TIA and the reconstitution of a tumor tissue hierarchy of differentiated cells. In an attempt to establish cell lines possessing CSC properties, we employed spheroid and adherent cultures of the cells derived from PLR59 and PLR123 xenografts in which $LGR5^+$ cells were enriched (over 10 passages). When cells derived from PLR59 and PLR123 were cultured as spheroids, their growth was rather slow, and the spheroids contained only a few $LGR5^+$ cells but more differentiated cells that were positive for CK20, which is a commonly used differentiation marker (Supporting Information Fig. S2). On the contrary, cells from PLR59 and PLR123 cultured under an adherent condition grew fast with a doubling time of approximately 2.5 days and showed epithelial morphology (Fig. 2B).

To examine TIA of the cells, subcutaneous injection of 10 cells from the spheroids formed tumors in 1 (PLR59-derived cells) or 2 (PLR123-derived cells) out of 6 injection sites (Supporting Information Table S2), whereas 10 cells from adherent cultures formed tumors in all six injection sites, and even a single cell injection of an adherent cell reconstituted tumors. Although the spheroid culture led to an increase in TIA as compared to that of the primary cells, the adherent culture was more efficiently enriched in cells possessing TIA. The histological morphology of the tumors from the adherent cells was almost the same as the original tumors (Fig. 2C). In addition, TIA of the adherent cells was maintained even after the cells were cultured for more than a month (Supporting Information Table S3).

We examined cell surface markers of the adherent cells from the PLR59 and PLR123 and found they were clearly positive for all known colon CSC markers reported earlier: $LGR5^+$, $ALDH^+$, $CD133^+$, $CD44^+$, $EpCAM^+$, $CD166^+$, $CD24^+$, $CD26^+$ and $CD29^+$ (Fig. 2D and Supporting Information Fig. S3). In addition, expression of the cell surface markers was unchanged even after one month of cell culture. One of the characteristics of CSCs is symmetrical cell division for self-renewal. The $LGR5^+$ adherent cells divided symmetrically under the adherent culture conditions (Fig. 2E). In the presence of matrigel and FBS, however, the $LGR5^+$ cells underwent asymmetrical cell divisions, as demonstrated by the segregation of LGR5 protein into one of two daughter cells (Fig. 2F), implicating the generation of two different offspring. Asymmetric cell divisions are one of the hallmarks of stem cells.

Colony forming activity and tumorigenicity of the sorted $LGR5^+$ and the $LGR5^-$ cells

In order to examine the ability of $LGR5^+$ and $LGR5^-$ cells to form colonies *in vitro* and tumors *in vivo*, we sorted the $LGR5^+$ and $LGR5^-$ populations from the primary cells of xenografts generated by the inoculation of the $LGR5^+$ cells. Anti-LGR5 antibody 2L36 was used for the cell sorting. About 93% of the cells in the $LGR5^+$ fraction were $LGR5^+$, and more than 99% of the cells in the $LGR5^-$ fraction were $LGR5^-$ (Fig.

3A). The sorted LGR5$^+$ cells but not the LGR5$^-$ cells efficiently formed colonies on matrigel *in vitro* and formed tumors in NOG mice. When 1,000 cells were subcutaneously injected into NOG mice, the sorted LGR5$^+$ cells formed large visible tumors by day 34 after the inoculation, but the LGR5$^-$ cells gave rise to only very tiny tumors by day 34 (Fig. 3B). We further examined the relation of LGR5 expression and other cancer stem cell markers by double staining the LGR5 with CD133, CD166 or CD44. Nearly all of the LGR5$^+$ cells were positive for CD133 and CD166, but there were large numbers of LGR5$^-$ cells that were positive for CD133 or CD166, indicating that LGR5 marks a subpopulation of CD133$^+$ and CD166$^+$ cells (Fig. 3C). Because significant numbers of LGR5$^+$/CD44$^-$ cells were present, CD44 does not mark all the LGR5$^+$ cells (Fig. 3C).

We employed cell sorting to further characterize the LGR5$^-$ cell populations. The cells from the xenografts were stained with the anti-LGR5 and anti-CD133 antibodies, and the LGR5$^-$/CD133$^-$, LGR5$^{-/low}$/CD133$^+$ and LGR5$^+$/CD133$^+$ cells were separated. More than 90% of the cells in each fraction were LGR5$^-$/CD133$^-$, LGR5$^{-/low}$/CD133$^+$ and LGR5$^+$/CD133$^+$ (Fig. 3D). The isolated LGR5$^+$/CD133$^+$ and LGR5$^{-/low}$/CD133$^+$ cells formed colonies on matrigel, whereas nearly all the LGR5$^-$ /CD133$^-$ cells died after seeding on culture plates; colony forming efficiency of the sorted LGR5$^-$ /CD133$^-$, LGR5$^{-/low}$/CD133$^+$ and LGR5$^+$/CD133$^+$ cells were about 0.03%, 1.6% and 4.3%, respectively (Fig. 3E and Supporting Information Fig. S4).

Interconversion between LGR5$^+$ proliferating and LGR5$^-$ drug resistant states

We next asked whether the LGR5$^+$ cells exhibited a drug resistant state, which is believed to be a typical characteristic of CSCs [37]. After treatment of the LGR5$^+$ cells with irinotecan for 3 days, the cells stopped proliferation and about half of the cells survived (Supporting Information Fig. S5). One hundred percent of the surviving cells became LGR5$^-$, but they retained other colon cancer stem cell markers (Fig. 4A, 4B and Supporting Information Fig. S6, Table S4). The LGR5$^-$ cells induced by treating the LGR5$^+$ cells with an anticancer drug were designated as drug resistant LGR5$^-$ cells in this study. LGR5$^-$ cells which were pre-existing in xenograft tissues and human tumor tissues are referred to as LGR5$^-$ cells. RT-qPCR for *LGR5*, *CD133*, *CD44*, *CD166* and *EPCAM* revealed that the *LGR5* mRNA was drastically decreased after irinotecan treatment, but the mRNAs of *CD133*, *CD44*, *CD166* and *EPCAM* did not decline or even increased after treatment (Supporting Information Fig. S7D). The mRNA level of *CK20* did not increase by the irinotecan treatment and remained at a low level (Supporting Information Fig. S2A). Although we cannot rule out the possibility that elimination of epitope by proteolytic cleavage on LGR5 occurred after irinotecan treatment, the cells that were not recognized by any of our anti-LGR5 antibodies were regarded as LGR5 negative. We examined the TIA of these drug resistant LGR5$^-$ cells. Even injection of the 10 LGR5$^-$ cells formed tumors in 2 sites (PLR59-derived cells) and the PLR123-derived cells formed tumors at one site out of 6 injection sites in the NOG mice (Supporting Information Table S5). Treatment of the LGR5$^+$ cells with 5-fluorouracil or oxaliplatin also gave rise to drug-resistant LGR5$^-$ cells which converted to an LGR5$^+$ state after re-seeding and culturing in the absence of the drugs (Supporting Information Fig. S8).

The drug resistant LGR5$^-$ cells did not grow even after irinotecan was removed from the culture medium (Supporting Information Fig. S5C). However, they became positive for LGR5 and resumed proliferation after re-plating (Fig. 4A, 4B). The transition from the LGR5$^+$ state to an LGR5$^-$ state and vice versa was also confirmed by observations with single cells in culture. When single LGR5$^+$ cells were cultured in multiwell plates, the cells transitioned to an LGR5$^-$ state within 3 days after irinotecan treatment. When single LGR5$^-$ cells that had been treated with irinotecan were then cultured in multiwell plates without irinotecan, 19 to 43% of the cells converted to the LGR5$^+$ state within

4 days (Fig. 4C and Supporting Information Table S6). In order to confirm proliferation of the $LGR5^+$ and drug resistant $LGR5^-$ cells, we also employed double staining of LGR5 and Ki67 with the *in vitro* cultures of the $LGR5^+$ and the $LGR5^-$ cells. The expression of LGR5 correlated well with Ki67 staining: the $LGR5^+$ cells were positive for Ki67, and the drug resistant $LGR5^-$ cells were negative for Ki67 (Fig. 4D).

Pathway analysis using the results of DNA microarray of both proliferating $LGR5^+$ and drug resistant $LGR5^-$ cells revealed characteristics of two distinct states. As expected from the growth status of the cells, genes involved in cell cycle were downregulated whereas genes in the p53 signaling pathway were upregulated in the drug resistant $LGR5^-$ cells (Supporting Information Fig. S9). Genes whose mRNA expression increased in the $LGR5^+$ cells included those involved in cell growth such as *LGR5*, *FGFBP1*, *FGFR4*, *ROR1*, *NFIA*, *PIGU*, *LPAR3* and *FZD2* (Supporting Information Fig. S7C).

Reconstitution of the epithelial cell type tumor hierarchy from $LGR5^+$ cells

The observations that the cells converted from the $LGR5^+$ to the drug resistant $LGR5^-$ state *in vitro* and that the drug resistant $LGR5^-$ cells formed tumors *in vivo* prompted us to examine whether the drug resistant $LGR5^-$ cells directly generate a tumor hierarchy of differentiated cell types or first convert to the $LGR5^+$ state *in vivo*. To detect drug resistant $LGR5^-$ cells, we attempted to identify the genes that are upregulated in the drug resistant $LGR5^-$ cells by comparing the gene expression profiles of the drug resistant $LGR5^-$ cells, the $LGR5^+$ cells, and the primary cells from the xenografts. From the gene expression analyses of DNA microarray, a heat map is shown (Fig. 5A and Supporting Information Fig. S7) for the top 20 genes encoding membrane proteins with the largest change. Genes whose mRNA expression was increased in the drug resistant $LGR5^-$ cells include MHC class II related genes (*HLA-DMA*, *HLA-DMB*), adhesion molecules related genes (*AMIGO2*, *FLRT3*, *GJB5*, *CLDN1*), G-protein coupled receptor protein signaling pathway related genes (*GPR87*, *GPR110*, *GPR172B*, *GNAI1*, *ABCA1*) and immune signaling related genes (*TNFSF15*, *BLNK*, *FAS*, *TMEM173*). We further evaluated the genes for which antibodies against their proteins are available (Supporting Information Table S7).

Immunohistochemical staining of the cells cultured *in vitro* with antibodies confirmed that HLA-DMA was rather specifically expressed in the drug resistant $LGR5^-$ cells (Fig. 5B). HLA-DMA was located in intracellular vesicles, and therefore, it cannot be used for cell sorting. Nevertheless, HLA-DMA can be a useful molecule for identifying the $LGR5^-$ cells in xenografts and also in clinical specimens. Because HLA-DMA is also expressed in macrophages, we also looked for genes that were expressed in both $LGR5^+$ and drug resistant $LGR5^-$ cells and identified EREG (Fig. 5A). Immunohistochemical staining with a monoclonal antibody against EREG confirmed the EREG expression in $LGR5^+$ and $LGR5^-$ cells (Fig. 5B and Supporting Information Fig. S10). By combination of these markers, $LGR5^-$ cells can be detected as HLA-DMA and EREG double positive cells. After injection of a homogenous population of drug resistant $LGR5^-$ cells into NOG mice, cells weakly expressing LGR5 but still positive for HLA-DMA and EREG appeared within 1 day after the injection, and then the $LGR5^+/EREG^+$ cells which were negative for HLA-DMA emerged by day 5 (Fig. 5C). The reconstitution of the epithelial tumor hierarchy of diverse cell types from the drug resistant $LGR5^-$ cells through transition to $LGR5^+$ cells was confirmed (Fig. 5D).

We next examined the possibility of a conversion of $LGR5^+$ cells to a drug resistant state *in vivo*. NOG mice bearing tumors derived from the $LGR5^+$ cells were administered intraperitoneally with a MTD dose (120 mg/kg) of irinotecan. Tumor growth was nearly completely inhibited (Fig. 5E) and ductal structures were heavily destroyed (Fig. 5F).

Under such conditions, the $LGR5^+$ cells were markedly decreased (Fig. 5F and Supporting Information Fig. S11). There was a significant increase in HLA-DMA-positive cells, which are $LGR5^-$, after irinotecan treatment. In contrast, about one-third of the cancer cells in both ducts and budding regions were $LGR5^+$ in the vehicle-treated control mice. Both $LGR5^+$ cells and $HLA\text{-}DMA^+/LGR5^-$ cells were positive for EREG (Fig. 5F). The $LGR5^+$ cells reappeared after termination of irinotecan treatment (Fig. 5F and Supporting Information Fig. S11). We also performed double staining with Ki67 and LGR5 or HLA-DMA that marks $LGR5^-$ CSCs. As in the *in vitro* cultured cells, there was a good correlation of LGR5 expression and Ki67 staining of the cells in the xenografts. The $LGR5^+$ cells were positive for Ki67, and the $LGR5^-/HLA\text{-}DMA^+$ cells were negative for Ki67 (Fig. 5G). Thus, tumor reconstitution occurred through the $LGR5^+$ cells.

Possible therapeutic application of anti-EREG antibody

EREG is expressed on the surface of both $LGR5^+$ and drug resistant $LGR5^-/HLA\text{-}DMA^+$ cells, but its expression is very low or hardly detectable in differentiated tumor cells and normal tissues (Fig. 5A and Supporting Information Fig. S12A). Therefore, EREG may be a potential therapeutic target. We first examined the growth inhibitory activity and ADCC activity of the anti-EREG antibody. The anti-EREG antibody induced ADCC activity against both $LGR5^+$ and drug resistant $LGR5^-$ cells in the presence of human PBMC that contained effector cells, such as NK cells and monocytes, but the antibody did not directly affect the growth of $LGR5^+$ and drug resistant $LGR5^-$ cells in the absence of effector cells *in vitro* (Supporting Information Fig. S12B, S12C). To test the expression of EREG *in vivo*, we subcutaneously inoculated the $LGR5^+$ cells into NOG mice in which EREG was highly expressed during early stages of tumor development, and later its expression was rather restricted to budding areas as compared to ducts when tumors formed clear duct structures. EREG positive cells were also detected after the mice bearing the tumors were administered irinotecan (Fig. 5F). Therefore, we tested the antitumor activity of the anti-EREG antibody after irinotecan treatment. SCID mice were used as a model for efficacy evaluation, because the antibody requires effector cells to elicit ADCC. When the antibody was administered at day 4 and day 11 after the final administration of irinotecan, it only delayed the tumor growth (Supporting Information Fig. S12D).

To test the efficacy in a metastatic model, we first examined the expression of EREG in metastasized tumors. When the $LGR5^+$ cells were intravenously injected into NOG mice, tumors were developed in several organs including the lung. For the tumors that developed in the lung, the majority of tumor cells were EREG positive (Fig. 6A). Efficacy was then tested using SCID-Beige mice in which macrophages and monocytes can serve as effectors for ADCC. When the antibody was administered once a week for 5 times starting 3 days after the tumor injection, the number of tumors at different sites was significantly decreased as compared to the control mice (Fig. 6B). In addition, the size of each tumor was also markedly reduced in the antibody treated mice (Fig. 6C, 6D).

The existence of both $LGR5^+$ and $LGR5^-$ cells in human colon cancers

We asked whether $LGR5^+$ and $LGR5^-$ cells could be detected in tissue sections of clinical colon cancers. Although rare, the $LGR5^+$ cells and the $LGR5^-$ cells which were $HLA\text{-}DMA^+/EREG^+$ were present in primary and metastatic colon cancer tissues from patients (Fig. 7A). Among 12 human colon cancer tissues, both $LGR5^+$ cells and $LGR5^-$ cells were detected in 8 cases, and either $LGR5^+$ or $LGR5^-$ cells were observed in the remaining 4 cases. The percentages of the $LGR5^+$ and $LGR5^-$ cells in those cases ranged between 0.003-1.864% for the $LGR5^+$ and 0.001-0.243% for the $LGR5^-$ cells (Supporting Information Table S8). Both $LGR5^+$ and $LGR5^-$ cells were detected in ducts and budding areas

(Fig. 7A and Supporting Information Table S8). In addition, $LGR5^+$ and $LGR5^-$ cells within the ducts were not restricted to particular regions as they were observed randomly throughout the ducts (Fig. 7A). In budding areas, $LGR5^+$ cells were detected as a single cell or in tumor cell clusters consisting of a few tumor cells (Fig. 7A). Also in clinical specimens, the $LGR5^+$ cells were positive for Ki67, and the $LGR5^-$/HLA-DMA^+ cells were negative for Ki67 (Fig. 7B).

DISCUSSION

Stem cell markers such as CD133, CD44, CD166 and ALDH have been used to identify and isolate colon CSCs [25-29]. We observed that colon CSCs reside in sub-populations of the cells positive for these markers; however, none is a definitive marker for colon CSCs. Evidence that Lgr5 marks normal intestinal SCs has accumulated [8, 13]. Despite that evidence, LGR5 remains unexplored in human CSCs, presumably due to a lack of specific antibodies [38]. In the present study, we generated monoclonal antibodies that are highly specific to LGR5 and can be applied to immunostaining, flow cytometry and cell sorting. Using these unique anti-LGR5 antibodies, we were able to define $LGR5^+$ cells as proliferating colon CSCs. To establish pure CSC cell lines, we tested whether spheroid cultures or adherent cultures would be useful to enrich CSCs. Several attempts have been made using spheroid cultures to isolate and enrich CSCs *in vitro* [9, 14]. The results in this study indicated that spheroid cultures allowed $LGR5^+$ cells to self renew and differentiate, leading to heterogeneous populations of cells as reported by others [14, 39]. In contrast, adherent cultures kept the $LGR5^+$ cells self renewing and prevented them from differentiation. Indeed, we did not detect any CK20 expression on the $LGR5^+$ cells during the culture. Thus, the $LGR5^+$ cell lines form a highly homogenous population of cells having CSC properties with strong TIA. Only a few previous reports have described the use of adherent cultures to obtain CSCs such as in glioma and breast cancers [30, 40, 41]. The adherent cultures were re-highlighted to isolate stable cell lines with CSC properties in this study.

Using the established $LGR5^+$ cell lines, definitive evidence for drug resistant $LGR5^-$ CSC subpopulations was obtained after treatment with anti-cancer drugs such as irinotecan. The $LGR5^+$ cells had a number of CSC characteristics such as self renewal via symmetric and asymmetric division, TIA, and a pathway for producing a tumor hierarchy of different cell types. In addition, these cell lines transition between two distinct states, an $LGR5^+$ proliferating and an $LGR5^-$ drug resistant state. Tumor formation from the drug resistant $LGR5^-$ cells in NOG mice was observed, but the TIA of the drug resistant $LGR5^-$ cells was slightly lower than that of $LGR5^+$ cells. Drug resistant $LGR5^-$ cells first converted to $LGR5^+$ cells in the establishment of tumor hierarchy *in vivo*. The results of irinotecan treatment *in vivo* suggest that anticancer drugs induce transition of $LGR5^+$ cells to drug resistant cells, and such drug resistant cells revert to $LGR5^+$ cells after drug treatment is terminated. We could detect both $LGR5^+$ and $LGR5^-$ cells in ducts and budding sites of the tumors reconstituted from either the $LGR5^-$ or $LGR5^+$ cells in mice and also in primary and liver metastasized tumors from patients. These observations may explain why some rare populations of cancer stem cells survive after drug treatments, giving rise to tumor recurrence. If this idea is correct, the CSC cell lines provide a new avenue to test drugs that will kill all of the cancer cells in a tumor.

CSCs self-renew and also give rise to differentiated cancer cells. In fact, the $LGR5^+$ cells exhibited the ability to undergo asymmetric cell divisions, generating two different offspring *in vitro* and reconstituting tumor hierarchy *in vivo*. However, it remains unclear whether a transition of differentiated cancer cells to CSCs occurs. Gupta et al. proposed a stochastic state transition of cancer cells [42]. Using breast cancer cell lines, they demonstrated that differentiated cancer cells possessed plasticity

and transitioned to CSCs to maintain phenotypic proportions within tumors, although the frequency was very low (between 0.01 and 0.1%). In this study, the colony forming activity of the sorted cells in the 99.4% pure $LGR5^-$ /$CD133^-$ population, in which almost all the cells are CSC marker-negative and thereby considered to be differentiated tumor cells, was approximately 0.03%. This number is extremely low but not zero. Therefore, the possibility of a reversion of differentiated cells to CSCs, as proposed by Gupta et al., cannot be ruled out. At the same time, the possibility that colonies were formed by a small number of concomitant $LGR5^+$ cells in this faction also cannot be excluded. Further study which overcomes technological hurdles of cell sorting is necessary to answer this question.

In normal small intestine, the existence of two types of SCs has been described: slow cycling SCs in the +4 position and proliferating SCs in the crypt base [43]. However, the relationship between the two types of SCs was unclear. More recently, $Lgr5^-$/$Bmi1^+$ SCs were shown to serve as a SC pool: they changed to $Lgr5^+$ SCs when the $Lgr5^+$ SCs were absent [15]. Furthermore, Takeda et al demonstrated the interconversion and bi-directional lineage relationship between proliferating $Lgr5^+$ SCs at the crypt base column and slow cycling SCs that expressed an atypical homeobox protein Hopx at +4 position [16]. Tert, telomerase reverse transcriptase, was reported as molecules that mark predominately noncycling, long lived intestinal SCs that proliferate upon injury [44]. Powell et al. also demonstrated that expression of Lrig1, a pan ErbB inhibitor, was rather specific to quiescent SCs [45]. However, Wong et al. indicated the coexpression of Lrig1 in $Lgr5^+$ cells [46], and intensive analysis with DNA microarray and proteomics revealed that Bmi1, Tert, Hopx and Lrig1 were all robustly expressed in $Lgr5^+$ intestinal stem cells [47]. In our RT-qPCR analysis, the *HOPX* mRNA was not detected in the $LGR5^+$ and drug resistant $LGR5^-$ cells, whereas similar levels of the *BMI1* and *LRIG1* mRNA were detected in both $LGR5^+$ and drug resistant $LGR5^-$ states (Supporting Information Fig. S13). In addition, expression of *TERT* was rather specific to the $LGR5^+$ cells; there was a marked decrease of the *TERT* mRNA after the $LGR5^+$ cells were treated with irinotecan (Supporting Information Fig. S13), which coincided with the results that intestinal stem cells contained significant telomerase activity [48]. Except for *HOPX* mRNA expression, we observed expression of the *BMI1*, *LRIG1* and *TERT* mRNAs in proliferating colon CSCs. Definitive understanding of the physiological roles and the expression of these genes in normal and cancer SCs await further study.

Because localization of proliferating ($Lgr5^+$) and slow cycling quiescent ($Lgr5^-$) SCs is restricted in normal intestine as described above, localization, proliferation, and transition between the slow cycling and proliferating states of SCs may be controlled by niches which include a gradient of the Wnt ligand [43]. The moderately differentiated colon cancers differed from the normal architecture: it showed duct structures and an epithelial hierarchy, but localization of $LGR5^+$ and $LGR5^-$ cells in ducts appeared not to be restricted to particular regions in both xenotransplanted tumors and in colon cancer tissues in patients, and they were observed throughout ducts. Thus, it seems that in tumor tissues, CSCs undergo proliferation and interconversion of their states without the underlying architecture of gradient producing cells at specific locations in the tissue structure.

It is widely believed that the invasive ability of cancer cells is important for metastasis. In addition, tumor budding is suggested to contribute to metastasis in colon cancer [49]. We could identify 3 markers--LGR5, HLA-DMA, and EREG--that can mark these CSCs in two distinct states. Because both proliferating and drug-resistant colon CSCs were EREG positive, we addressed whether anti-EREG antibody is efficacious against tumor metastasis. The antibody showed only moderate activity against the established xenograft tumors, but exhibited a stronger efficacy in a metastatic model tested in

this study, suggesting that the anti-EREG antibody is efficacious in the early stage of cancer development when cancers are rich in CSCs. A number of studies suggest that metastatic nodules arise from rare cells in the primary tumor (CSCs) [50]. If this is correct, then therapies targeting CSCs can have profound effects against metastatic tumors, even greater than upon primary tumors. In this way the CSC cell lines developed here can give rise to novel therapies that could improve the treatment of cancer patients.

During the review process for this article, three papers appeared providing the evidence for the existence of CSCs in solid tumors in mice: Chen J. et al. (NATURE 2012: 488: 522-526), Driessens G. et al. (NATURE 2012: 488: 527-530), and Schepers AG. et al. (SCIENCE 2012: 337: 730-735).

CONCLUSION

We established human colon cancer cell lines that express LGR5 and possess CSC properties. After treatment of the proliferating $LGR5^+$ cells with an anticancer agent, the $LGR5^+$ cells transition to a drug-resistant $LGR5^-$ state. In addition, the $LGR5^-$ cells converted to an $LGR5^+$ state in the absence of the drug, suggesting a pool of stem cells with the ability to interconvert between two distinct states. Using antibodies against LGR5, HLA-DMA and EREG, we show the existence of $LGR5^+$ and $LGR5^-$ cells in xenotransplanted tumor tissues and in human colon cancer tissues from patients. Furthermore, the anti-EREG antibody exhibited antitumor activity against tumors derived from the $LGR5^+$ cells in a metastatic model. This suggests the physiological importance of CSCs in tumor recurrence. Further, using the anti-EREG antibody, we provide an option for cancer stem cell targeting therapy.

ACKNOWLEDGMENTS

We thank L. C. Wong, G. N. Yeow, H. S. Ong, Z. X. Wong, and Y. Takai for their technical assistance, Y. Ohnishi, E. Fujii, K. Nakano and K F-Ouchi for critical discussions, and R. Somerville for proof editing the manuscript. Thanks are also to T. Yamamura and R. Nomura for their continuous support throughout the study. We are also grateful to Mr. O. Nagayama, CEO of Chugai, for his encouragement. This work is supported in part by a grant from Singapore Economic Development Board.

Disclosure of potential conflicts of interest

S.K., H.Y.O., M.S., O.N., A.K., K.M., M.Y., S.F., K.Y., E.H., Y.W., H.M., M.A., C.K., T.W., T.Yo and T.Ya. are employees of Chugai Pharmaceutical Co., Ltd. Y.J.C. is employee of PharmaLogicals Research Pte. Ltd. The authors indicate no other potential conflict of interest.

REFERENCES

1. Shackleton M, Quintana E, Fearon ER, et al. Heterogeneity in cancer: cancer stem cells versus clonal evolution. CELL 2009;138:822-829.
2. Clevers H. The cancer stem cell: premises, promises and challenges. NAT MED 2011;17:313-319.
3. Vaiopoulos AG, Kostakis ID, Koutsilieris M, et al. Concise review: Colorectal cancer stem cells. STEM CELLS 2012;30:363-371.
4. Nguyen LV, Vanner R, Dirks P, et al. Cancer stem cells: an evolving concept. NAT REV CANCER 2012;12:133-143.
5. Marusyk A, Almendro V, Polyak K. Intra-tumour heterogeneity: a looking glass for cancer? NAT REV CANCER 2012;12:323-334.
6. Visvader JE, Lindeman GJ. Cancer stem cells: current status and evolving complexities. CELL STEM CELL 2012;10:717-728.
7. Magee JA, Piskounova E, Morrison SJ. Cancer stem cells: impact, heterogeneity, and uncertainty. CANCER CELL 2012;21:283-296.
8. Barker N, Ridgway RA, van Es JH, et al. Crypt stem cells as the cells-of-origin of intestinal cancer. NATURE 2009;457:608-611.
9. Vermeulen L, Todaro M, de Sousa Mello F, et al. Single-cell cloning of colon cancer stem cells reveals a multi-lineage differentiation capacity. PROC NATL ACAD SCI U S A 2008;105:13427-13432.

10. Takahashi H, Ishii H, Nishida N, et al. Significance of Lgr5(+ve) cancer stem cells in the colon and rectum. ANN SURG ONCOL 2011;18:1166-1174.
11. Takeda K, Kinoshita I, Shimizu Y, et al. Expression of LGR5, an intestinal stem cell marker, during each stage of colorectal tumorigenesis. ANTICANCER RES 2011;31:263-270.
12. Walker F, Zhang HH, Odorizzi A, et al. LGR5 is a negative regulator of tumourigenicity, antagonizes Wnt signalling and regulates cell adhesion in colorectal cancer cell lines. PLOS ONE 2011;6:e22733.
13. Barker N, van Es JH, Kuipers J, et al. Identification of stem cells in small intestine and colon by marker gene Lgr5. NATURE 2007;449:1003-1007.
14. Vermeulen L, De Sousa E Melo F, van der Heijden M, et al. Wnt activity defines colon cancer stem cells and is regulated by the microenvironment. NAT CELL BIOL 2010;12:468-476.
15. Tian H, Biehs B, Warming S, et al. A reserve stem cell population in small intestine renders Lgr5-positive cells dispensable. NATURE 2011;478:255-259.
16. Takeda N, Jain R, LeBoeuf MR, et al. Interconversion between intestinal stem cell populations in distinct niches. SCIENCE 2011;334:1420-1424.
17. Quintana E, Shackleton M, Foster HR, et al. Phenotypic heterogeneity among tumorigenic melanoma cells from patients that is reversible and not hierarchically organized. CANCER CELL 2010;18:510-523.
18. Sharma SV, Lee DY, Li B, at al. A chromatin-mediated reversible drug-tolerant state in cancer cell subpopulations. CELL 2010;141:69-80.
19. Roesch A, Fukunaga-Kalabis M, Schmidt EC, et al. A temporarily distinct subpopulation of slow-cycling melanoma cells is required for continuous tumor growth. CELL 2010;141:583-594.
20. Gupta PB, Fillmore CM, Jiang G, et al. Stochastic state transitions give rise to phenotypic equilibrium in populations of cancer cells. CELL 2011;146:633-644.
21. Dieter SM, Ball CR, Hoffmann CM, et al. Distinct types of tumor-initiating cells form human colon cancer tumors and metastases. CELL STEM CELL 2011;9:357-365.
22. Lapidot T, Sirard C, Vormoor J, et al. A cell initiating human acute myeloid leukaemia after transplantation into SCID mice. NATURE 1994;367:645-648.
23. Al-Hajj M, Wicha MS, Benito-Hernandez A, et al. Prospective identification of tumorigenic breast cancer cells. PROC NATL ACAD SCI U S A 2003;100:3983-3988.
24. Singh SK, Hawkins C, Clarke ID, et al. Identification of human brain tumour initiating cells. NATURE 2004;432:396-401.
25. O'Brien CA, Pollett A, Gallinger S, et al. A human colon cancer cell capable of initiating tumour growth in immunodeficient mice. NATURE 2007;445:106-110.
26. Ricci-Vitiani L, Lombardi DG, Pilozzi E, et al. Identification and expansion of human colon-cancer-initiating cells. NATURE 2007;445:111-115.
27. Dalerba P, Dylla SJ, Park IK, et al. Phenotypic characterization of human colorectal cancer stem cells. PROC NATL ACAD SCI U S A 2007;104:10158-10163.
28. Huang EH, Hynes MJ, Zhang T, et al. Aldehyde dehydrogenase 1 is a marker for normal and malignant human colonic stem cells (SC) and tracks SC overpopulation during colon tumorigenesis. CANCER RES 2009;69:3382-3389.
29. Chu P, Clanton DJ, Snipas TS, et al. Characterization of a subpopulation of colon cancer cells with stem cell-like properties. INT J CANCER 2009;124:1312-1321.
30. Mather JP. Concise Review: Cancer Stem Cells: In Vitro Models. STEM CELLS 2012;30:95-99.
31. Kremer L, Marquez G. Generation of monoclonal antibodies against chemokine receptors. METHODS MOL BIOL 2004;239:243–260.
32. Todaro M, Alea MP, Di Stefano AB, et al. Colon cancer stem cells dictate tumor growth and resist cell death by production of interleukin-4. CELL STEM CELL 2007;1:389-402.
33. Hu Y, Smyth GK. ELDA: Extreme limiting dilution analysis for comparing depleted and enriched populations in stem cell and other assays. J IMMUNOL METHODS 2009;347:70-78.
34. Sato Y, Mukai K, Watanabe S, et al. The AMeX method. A simplified technique of tissue processing and paraffin embedding with improved preservation of antigens for immunostaining. AM J PATHOL 1986;125:431-435.
35. Suzuki M, Katsuyama K, Adachi K, et al. The combination of fixation using PLP fixative and embedding in paraffin by the AMeX method is useful for histochemical studies in assessment of immunotoxicity. J TOXICOL SCI 2002;27:165-172.
36. Fujii E, Suzuki M, Matsubara K, et al. Establishment and characterization of in vivo human tumor models in the NOD/SCID/gamma(c)(null) mouse. PATHOL INT 2008;58:559-567.
37. Buczacki S, Davies RJ, Winton DJ. Stem cells, quiescence and rectal carcinoma: an unexplored relationship and potential therapeutic target. BR J CANCER 2011;105:1253-1259.
38. Barker N, Bartfeld S, Clevers H. Tissue-resident adult stem cell populations of rapidly self-renewing organs. CELL STEM CELL 2010;7:656-670.
39. Emmink BL, Van Houdt WJ, Vries RG, et al. Differentiated human colorectal cancer cells protect tumor-initiating cells from irinotecan. GASTROENTEROLOGY 2011;141:269-278.
40. Pollard SM, Yoshikawa K, Clarke ID, et al. Glioma stem cell lines expanded in adherent culture have tumor-specific phenotypes and are suitable for chemical and genetic screens. CELL STEM CELL 2009;4:568-580.

41. Scheel C, Eaton EN, Li SH, et al. Paracrine and autocrine signals induce and maintain mesenchymal and stem cell states in the breast. CELL 2011;145:926-940.
42. Gupta PB, Fillmore CM, Jiang G, et al. Stochastic state transitions give rise to phenotypic equilibrium in populations of cancer cells. CELL 2011;146:633-644.
43. Li L, Clevers H. Coexistence of quiescent and active adult stem cells in mammals. SCIENCE 2010;327:542-545.
44. Montgomery RK, Carlone DL, Richmond CA, et al. Mouse telomerase reverse transcriptase (mTert) expression marks slowly cycling intestinal stem cells. PROC NATL ACAD SCI U S A 2011;108:179-184.
45. Powell AE, Wang Y, Li Y, et al. The pan-ErbB negative regulator Lrig1 is an intestinal stem cell marker that functions as a tumor suppressor. CELL 2012;149:146-158.
46. Wong VW, Stange DE, Page ME, et al. Lrig1 controls intestinal stem-cell homeostasis by negative regulation of ErbB signaling. NAT CELL BIOL 2012;14:401-408.
47. Muñoz J, Stange DE, Schepers AG, et al. The Lgr5 intestinal stem cell signature: robust expression of proposed quiescent '+4' cell markers. EMBO J 2012;31:3079-3091.
48. Schepers AG, Vries R, van den Born M, et al. Lgr5 intestinal stem cells have high telomerase activity and randomly segregate their chromosomes. EMBO J 2011;30:1104-1109.
49. Brabletz T, Jung A, Spaderna S, et al. Opinion: migrating cancer stem cells - an integrated concept of malignant tumour progression. NAT REV CANCER 2005;5:744-749.
50. Wu X, Northcott PA, Dubuc A, et al. Clonal selection drives genetic divergence of metastatic medulloblastoma. NATURE 2012;482:529-533.

See www.StemCells.com for supporting information available online.

Figure 1. Antigen specific binding of anti-LGR5 antibodies and characteristics of human colon cancer xenografts using NOG mice. (**A**): Regions of the LGR5 protein that contain epitopes of the anti-human LGR5 monoclonal antibodies, 2L36 and 2U2E-2. The monoclonal antibodies, 2L36 and 2U2E-2, were obtained by immunizing the *LGR5* cDNA and N-terminal region of the protein, respectively. Green bars correspond to the regions containing epitopes. (**B and C**): Specific binding of the anti-LGR5 antibodies to the antigen. (B) Immunocytochemistry of CHO DG44 cells transfected with the *LGR4*, *LGR5*, or *LGR6* cDNA. 2L36 and 2U2E-2 recognized the cells expressing LGR5 but not those expressing LGR4 or LGR6. (C) Flow cytometry analysis of CHO DG44 cells transfected with the *LGR4*, *LGR5*, or *LGR6* cDNA. 2L36 reacted with the cells expressing LGR5 but not those expressing LGR4 or LGR6. (**D**): Staining of the crypt base cells in normal human intestine. The thin sections of the normal human intestine were stained with 2U2E-2. Specific fluorescence was observed in the crypt base columnar cells (arrows). (**E**): Histology of surgically resected tumors of PLR59 and PLR123 and xenograft tumor tissues. Tumors derived from PLR59 and PLR123 had tubular structures containing goblet cells (inserts) and budding cluster (arrows). Bar: 50 μm. (**F**): Immunostaining of LGR5 in the surgically resected tumors (PLR123) and xenografts derived from PLR123. Sections were stained with the anti-LGR5 antibody. Bar: 25 μm. Original, surgically resected tumors from patients.